16TH EUROPEAN CONFERENCE ON EARTHQUAKE ENGINEERING THESSALONIKI 18 - 21 JUNE 2018

HYBRID FOUNDATIONS USED FOR PROTECTION AGAINST REVERSE FAULT RUPTURE

Marianna LOLI[1], Irene GEORGIOU[2], Evangelia GARINI[3], George GAZETAS[4]

ABSTRACT

Earthquakes of significant magnitude are often characterized by spectacular manifestations of the tectonic hazard. Surface reflections of the causative fault often interact with foundation–structure systems causing excessive permanent deformations and failure, even in cases of structures designed according to modern code requirements. Based on the well-established recognition that key to the survival of the structure under large fault offsets is the appropriate design of the foundation, this paper proposes foundation solutions that can retain their superior performance under the concurrent effect of strong shaking and fault rupture. A series of 1-g physical model tests were carried out to study the response of hybrid foundations combining: (i) a footing designed according to the principle of rocking isolation with (ii) a retaining-type below-ground construction that can divert the fault rupture and sufficiently confine the soil in the vicinity of the footing so as to limit permanent deformations. The response of such hybrid foundation – structure systems to thrust fault rupture propagating through a stratum of dense dry sand, as well as the response of the same structure without the foundation improvement, were tested using a custom made 3 m long split-box at a scale of 1 : 15. Two different locations of the structure relative to the fault were considered. A numerical method using three-dimensional finite elements was developed and validated through successful prediction of the physical model tests.

Keywords: Seismic design; Fault rupture; Physical modelling; Numerical analysis; Hybrid Foundations

1. INTRODUCTION

Historic earthquakes have provided numerous examples of the devastating effects of earthquake surface fault rupture on built environment (e.g. Chang et al., 2000; Youd et al., 2000; Kawashima, 2001; Dong et al., 2003; Pamuk et al., 2005; Faccioli et al., 2008). Although the traditional geotechnical design approach to tectonic displacements is avoidance, recent earthquakes have proved our imperfect understanding and our inability to predict tectonic movements. It is worth mentioning for example that all the events of the 2010–2011 Canterbury earthquake sequence (i.e. the 4 September 2010 M_w = 7.1 Darfield earthquake and the three subsequent earthquakes of $M_w \geq 5.9$) occurred on previously unknown faults.

The idea that, similar to other forms of ground failure, it is possible to develop effective design strategies to address the fault rupture hazard came thanks to the observation of some spectacular satisfactory performances among case studies of failures. In a notable number of cases, structures survived major fault offsets with hardly any damage. Comprehensive study of field observations followed by numerical analyses (Anastasopoulos and Gazetas, 2007) revealed an interplay taking place between the propagating fault rupture, the soil, the foundation, and the supported structure. Both analytical (Yilmaz & Paolucci, 2007; Paolucci & Yilmaz, 2008; Anastasopoulos et al., 2008; 2009) and experimental (Bransby et al., 2008; Ahmed & Bransby, 2009; Loli et al., 2011) results have shown that key to the survival of the structure is the appropriate design of the foundation, pointing towards bulk, continuous and rigid foundation systems (i.e. slab or box-type). The latter are capable of causing

[1]Postdoctoral Researcher, School of Civil Engineering, NTUA, Athens, Greece, mariannaloli@yahoo.com
[2]PhD Candidate, School of Civil Engineering, NTUA, Athens, Greece, irelimni @outlook.com
[3]Postdoctoral Researcher, School of Civil Engineering, NTUA, Athens, Greece, geocvemp@yahoo.gr
[4]Professor, School of Civil Engineering, NTUA, Athens, Greece, gazetas@central.ntua.gr

total or partial diversion and/or diffusion of the fault and can therefore significantly reduce permanent deformations imposed upon the structure. Alternatively, in cases of already known faults, mitigation strategies may include construction of a soft deformable wall barrier (such as a bentonite wall) between the structure and the rupture path (Fadaee et al., 2016).

However, it goes without saying that tectonic movements are accompanied by strong ground shaking, which can be especially severe in the near-fault region. It is therefore necessary to propose mitigation measures that will effectively shield the structure against both the tectonic as well as the dynamic component of seismic hazard. Despite their admittedly superior performance when interacting with a propagating fault rupture, rigid, bulky foundations impose extreme demands for ductility of the above-ground structural elements for inertial loads to be safely undertaken. In fact, current research results on the mechanisms of shallow foundation response promote the opposite design notion. They suggest under-designing foundations in order to promote nonlinear rocking oscillations and thereby isolate the superstructure (rocking isolation) especially against extreme seismic demands (Gajan & Kutter, 2009; Deng et al. 2011; Anastasopoulos et al., 2011; Gelagoti et al., 2012; Loli et al., 2014).

Aiming to resolve this contradiction, the present study investigates the interaction between reverse fault rupture and hybrid foundations involving a rocking isolated, under-designed, footing with bellow ground diaphragm wall-type constructions built to confine the soil around the footing and therefore improve its ability to resist permanent deformations. Results from 1-g physical model tests of 1 : 15 foundations supported on dense sand are accompanied by a parametric study using validated 3-D FE models.

2. PROBLEM DEFINITION

Figure 1 indicates schematically the main features of the studied prototype problem. A square B x B (B = 2.1 m) shallow foundation sits atop a layer of dense dry ($D_r \approx 80\%$) sand. The footing carries a vertical dead weight pressure (q) determined with respect to the foundation capacity in order to achieve a realistic factor of safety in vertical loading ($FS_V = 5.6$). Foundation improvement consists of a cofferdam structure with plan area (B_c x B_c) and depth D. It should be noted that, according to dynamic centrifuge test results (Loli, 2015), such a hybrid foundation solution constitutes a particularly effective means of combining the virtues of rocking isolation with uplift dominated response and hence limited permanent displacements.

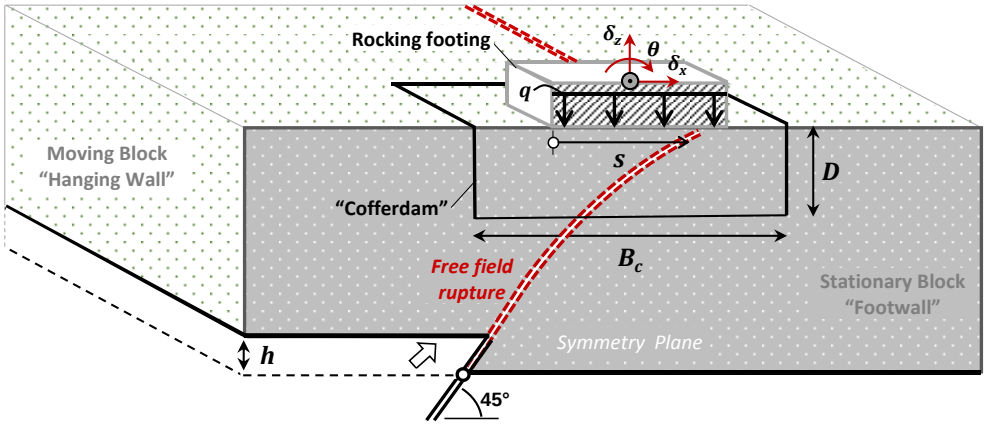

Figure 1. Schematic of the studied problem: response of a hybrid foundation combining a rocking isolated footing with below-ground improvement (cofferdam). Note that only half of the problem geometry is sketched taking advantage of the highlighted symmetry plane.

Reverse fault displacement of vertical amplitude h, dipping at 45°, is applied at the bedrock. The hanging wall (displaced block) moves upwards while the footwall remains stationary. In free field conditions, fault deformation localizes upon a single shear band (fault rupture) and the relative to the

fault location of the structure is herein defined with respect to parameter s, which is the horizontal distance between the free field fault scarp and the hanging wall corner of the footing (generally normalized by the foundation width). The foundation moves as a rigid body and its movement will hereafter be quantified by the rotation θ and the displacement vector δ (δ_x and δ_z, referring to the horizontal and the vertical component, respectively) measured at the middle point.

3. METHODOLOGY

3.1 Physical Modelling

The experimental program made use of a custom-built split box with internal dimensions 2.6 x 1.1 x 1.0 m (length x width x height). This apparatus is equipped with a fixed and a movable part; the latter is electronically controlled and can translate down/outwards to simulate normal faulting (i.e., extension), or up/inwards to simulate thrust faulting (i.e., compression). Fault deformation is applied at a controllable speed, in a quasi-static manner, reaching base dislocations of up to 1/10 of the soil model depth. The two longitudinal sides of the split-box are transparent to allow visual observation of soil deformations and Figure 2 displays a side view of the model containing the cofferdam improvement.

A global scaling factor N = 15 was selected for this study and all physical properties were scaled down according to similitude laws governing 1-g model testing (Muir Wood, 2004). The testing program involved a total of four physical model tests, one studying the propagation of fault rupture in the free field (i.e. in absence of structures) and three involving fault–foundation–structure interaction, were conducted at the Laboratory of Soil Mechanics of the National Technical University of Athens. The size of the footing model (B = 0.14 m) in comparison to the out-of-plane width of the split box (1.1 m) allowed modelling two foundation¬structure models at the same time without any considerable interaction between them. The two models were placed at the same location relative to the fault and opposite to each other, each one facing one of the transparent sides of the box. Thanks to this configuration, every test, aside from the free field one, studied simultaneously the response of the shallow foundation (benchmark case) and the response of the "improved" hybrid foundation enabling direct comparison of the two systems. It should be noted that, the Perspex acts as a symmetry plane and therefore only half of the foundation–structure system out-of-plane geometry is modelled.

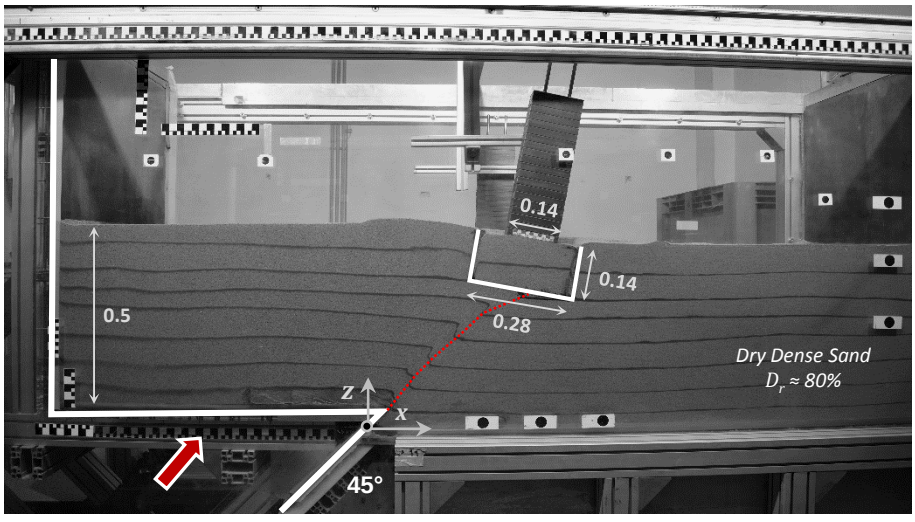

Figure 2. Photo of the physical model in the split-box indicating key dimensions in meters.

A dry, industrially produced, fine quartz sand with D_{50} = 0.15 mm and uniformity coefficient $C_u = D_{60}/D_{10}$ = 2.5, was used in the experiments. The 0.5 m deep soil model was prepared using an electronically-controlled sand raining system designed to produce soil samples of controllable relative

density ensuring repeatability (Drosos et al., 2012). The response of the footing as well as that of the cofferdam were assumed to be elastic and these elements were made of steel and aluminium respectively. No attempt was made to reproduce the bending stiffness characteristics of the retaining walls presuming that they would practically respond as rigid bodies owing to their section stiffness being significantly greater than that of the adjacent soil under extreme shearing (fault rupture). Hence, 10 mm thick aluminum plates were used to construct the cofferdam and the skirt. Sandpaper was glued at the bottom-side of the footing to reproduce realistic concrete – soil interface friction properties. On the other hand, the aluminum plates consisting the cofferdam and skirt walls were smooth with assumed friction coefficient $\mu = 0.3$.

Former studies (e.g. Bransby et al., 2008; Anastasopoulos et al., 2009) have shown the significant effect of the foundation bearing pressure on the mechanisms of fault rupture–foundation interaction. Therefore, although structural properties are not modelled in this study, it was considered necessary to retain the bearing pressure carried by the foundation at a realistic level. A factor of safety FS_V representative of a footing designed according to rocking isolation (here the considered value is FS_V = 5.6) was selected and the required bearing pressure was calculated with respect to traditional bearing capacity formulas (Meyerhof, 1951) for soil friction angle equal to its critical state value $\varphi_{cs} = 32^0$. The required bearing pressure was imposed by attaching on top of the foundation steel plates of the same plan area.

A pair of digital cameras was used to take pictures of the model from a fixed position on either Perspex side of the box. Approximately 50 pictures per test were taken at progressively increasing fault displacements. The photographic data were then analyzed using the Geo-PIV program, written by White et al. (2003), to calculate foundation displacements and the shear strains developed within the soil. The latter was facilitated by the presence of narrow layers of colored sand amid the soil stratum.

3.2 Numerical Simulation

The numerical method proposed by Anastasopoulos et al. (2007) was implemented within the ABAQUS FE code. The same model has in the past been employed in simulations of the response of deep embedded foundations interacting with dip-slip faults (Loli et al., 2012) achieving excellent agreement with centrifuge model tests results.

The numerical model dimensions were chosen to be the same as the dimensions of the physical model at prototype scale. Figure 3 shows the FE mesh used in the analyses indicatively for the case that the structure is positioned at s =3.6 m and subjected to 1m of fault dislocation at the bedrock. Only half of the model was simulated, taking advantage of the symmetry along the center-line of the foundation (which corresponds to the location of the Perspex front face in the physical model models).

The sand was modelled with 8-noded hexahedral continuum finite elements. The elasto-plastic constitutive relation described by Anastasopoulos et al. (2007) was used and encoded in ABAQUS through a user subroutine. This assumes elastic pre-yield soil behavior defined by the secant shear modulus G. The Mohr–Coulomb failure criterion was used to define failure accompanied by an isotropic strain softening law, which degraded the friction (φ) and dilation (ψ) angles linearly with octahedral plastic shear strain γ^{pl}_{oct}. Model parameters were calibrated with respect to shear boc test results (Loli & Gazetas., 2017).

3-D continuum elements were also used to model the structural components (the footing, the structure, and the cofferdam) with assumed linearly elastic material response and typical stiffness properties of steel and aluminum. Soil–foundation interface was modelled using contact elements to allow sliding and/or detachment (loss of contact). A large enough coefficient of friction ($\mu = 0.7$) was assumed to be representative of the soil–footing interface, where sandpaper was used, while a lower value of 0.3 was used to simulate the frictional properties for the smooth aluminum walls of the cofferdam/skirt.

The bottom boundary represents the interface between soil layer and rigid bedrock. Hence, it is split in two parts, one that remains stationary and the other which follows the hanging wall movement of the fault. The analyses were conducted in three steps. Initially, the geostatic conditions (including application of soil self-weight) were activated in Step 1, followed by gravity loading (with the dead load of the footing and the superstructure) in Step 2. The differential fault displacement was then applied in Step 3 in adequately small, quasi-static analysis increments.

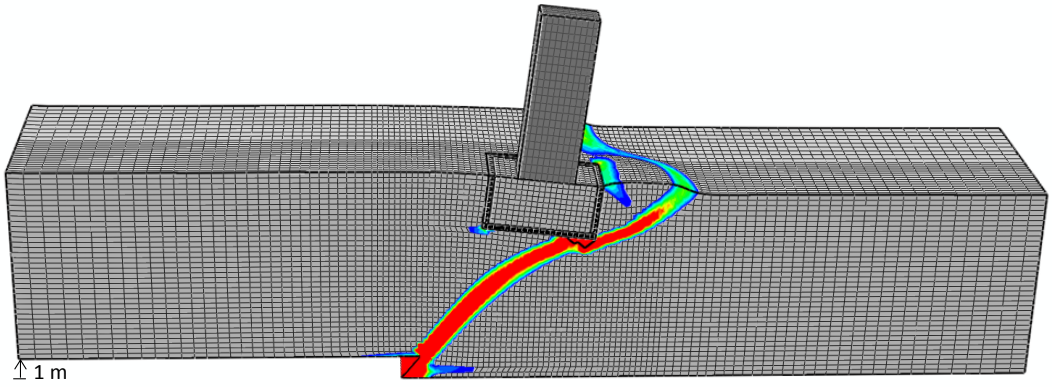

Figure 3. Snapshot of the deformed 3-D FE mesh.

4. ANALYTICAL VERSUS EXPERIMENTAL RESULSTS

The effectiveness of the hybrid foundation is discussed in this section through comparison of its response with the "unprotected" footing solution for two different (relative to the fault) locations. Class-A numerical predictions are also shown to demonstrate the validity of the numerical method. Unless otherwise stated, the following results are presented in prototype scale.

4.1 Location s/B = 1.2

In this position of the structure, the free field rupture would outcrop slightly further from the footing corner towards the footwall, leaving the entire structure on the hanging wall. Model images taken at 0.6 m of fault throw from either (footing/cofferdam) side of the split-box indicate that the presence of the structure modifies the rupture pattern in comparison to the free field (Figure 4a). Moreover, the rupture patterns observed for each foundation case are strikingly different.

In the case of the footing, the shear band initially follows the free field path. Yet, further propagation towards the surface with the same dipping angle is hindered due to the pressure field imposed by the footing. Fault bifurcation starts at about 1/3 of the soil depth and from this point two strands (L1, L2) propagate simultaneously towards the surface, each outcropping on either side of the footing. As a result, soil heaves of significant height form on both sides (see surface displacement plots in Figure 4b). They are indicative of extensive soil yielding taking place around the footing. Bearing capacity failure mechanisms are evidenced by the drastic increase of footing rotation for h > 0.4 m leading to total failure (overturning) for h = 0.6 m (Figure 4c).

The alternative, hybrid foundation system, shows generally superior performance. Similarly to the footing case, bedrock dislocation initially propagates along a fault plane which coincides with the free field plane (L1, Figure 4a). Yet, evolution of this rupture is prevented by the kinematic constraints imposed by the cofferdam bottom wall. Part of the fault dislocation is relieved through sliding of the moving-block soil along the cofferdam wall on the hanging wall side (L1'). The consequent cofferdam movement and clockwise rotation causes formation of a passive type failure wedge on its footwall side (L2'). This facilitates the development of a second rupture plane (L2) with a shallower dip angle which thereafter becomes the main fault. Surface displacement profiles (Figure 4b) indicate the formation of a soil bulge on the footwall side of the cofferdam due to the combined effect of passive-type soil wedge formation and the outcropping fault. The footing on top experiences significantly lower distress (about half rotational amplitudes) in comparison to the alternative without the cofferdam, avoiding collapse (Figure 4c).

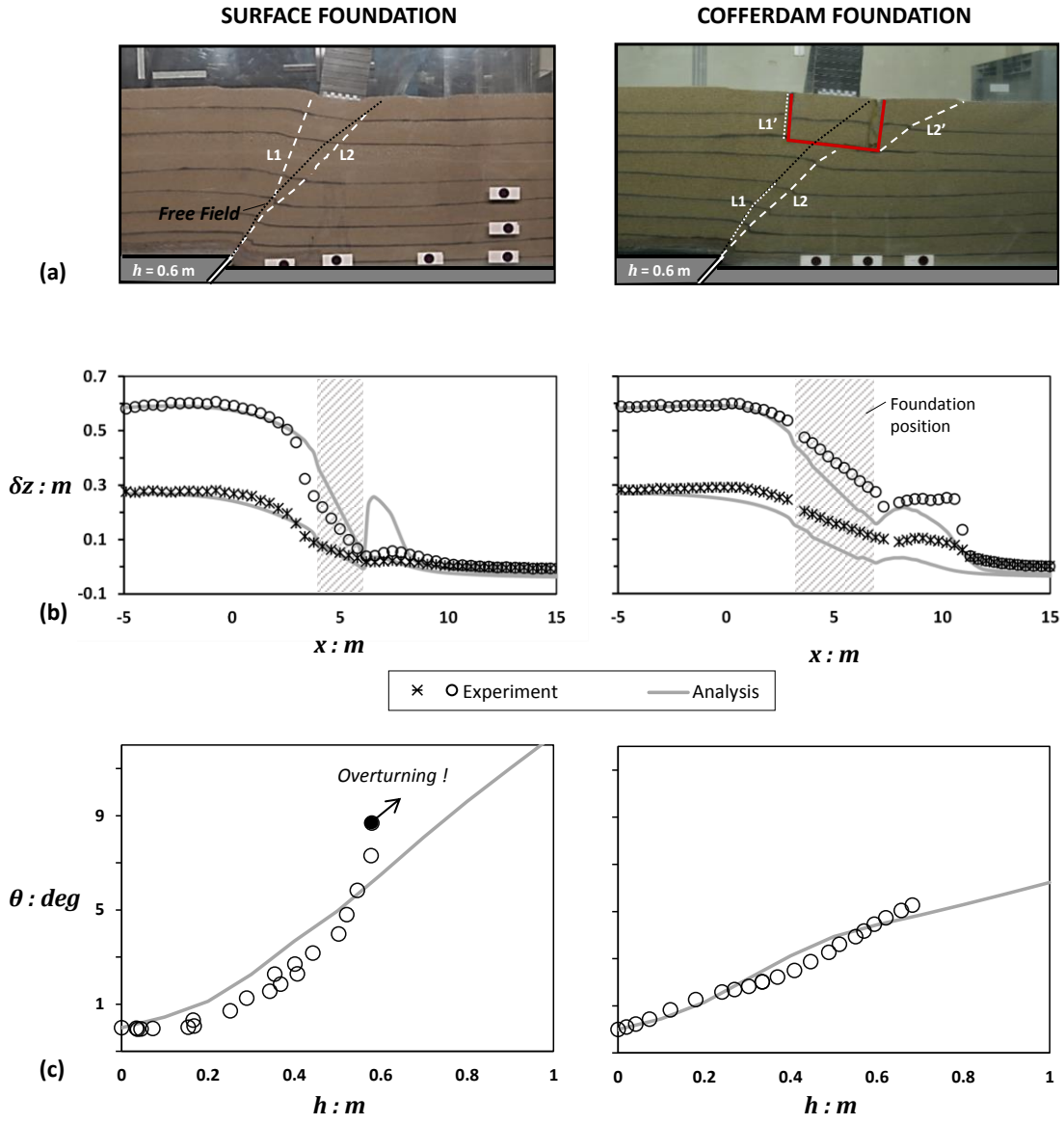

Figure 4. Response of a structure supported upon a hybrid footing–cofferdam foundation (right) in comparison to the benchmark surface foundation solution (left) for h = 0.6 m and relative to the fault position s/B = 1.2: (a) photos of the respective physical models; (b) experimental vs. analytical surface displacement profiles; and (c) evolution of foundation rotation in the experiment compared to the analysis.

Figures 4b and 4c demonstrate the general agreement between numerical predictions and experiment for both foundation types and throughout the entire range of examined throw values. The analysis successfully predicts the variety of fault rupture–foundation interaction mechanisms capturing the fault outcropping positions and the evolution of surface deformation patterns. Foundation rotation is predicted with remarkable accuracy for low fault amplitudes, yet underestimated at larger displacements. This was an expected outcome of the fact that the numerical analyses unavoidably ignore geometric non-linearity because the opposite has been proven to create severe numerical instabilities when combined with strain-softening user subroutine (Loli, 2015). As a result, the numerical model deliberately ignores P-δ effects (i.e. additional moment loading induced by the eccentricity of the structural center of mass as the footing rotates) in order to focus on the correct representation of soil response. Therefore, it consistently under-predicts footing rotations at large displacements (when eccentricity becomes important) capturing however the correct trend of comparative performance between the two systems.

4.1 Location s/B = 0.8

In this test the structure location was modified so that the free field path intersects with the footing base in the vicinity of its footwall side corner. Figure 5 summarizes test results and numerical predictions revealing, as in the previous case, important fault–foundation interaction mechanisms as well as a striking reversal of the previous comparative performance of the two foundation alternatives.
Designed according to the rocking isolation concept, the footing is too heavy (i.e. with a relatively low FS_V) to move upwards due to interaction with the fault. As in the previous position, the rupture (L1) follows its free field path in the bottom half of the soil depth. Yet, as it propagates further up, it deviates towards the hanging wall to avoid the "pain" of translating the heavy footing (Figure 5a). With a significant increase in the dipping angle, it deviates towards the hanging wall to emerge by the hanging wall side of the footing. As a result, the footing–structure is left on the stationary block of soil almost undisturbed, experiencing minimal translation and much less rotation in comparison to the previously discussed case (Figure 5c).
On the other hand, a fascinating interplay takes place between the fault and the cofferdam in the case of the hybrid foundation, which involves a variety of soil failure mechanisms (highlighted in Figure 5a). Two stages of faulting can be recognized: First, as previously, fault displacement initially propagates upon a rupture plane (L1) which follows the free field path until it meets the rigid constraint imposed by the bottom wall of the cofferdam. A diffused shearing zone forms around the bottom corner of the cofferdam on its hanging wall side while, further up, shearing localizes upon the soil–cofferdam interface (L1'). The cofferdam resists the movement of the hanging wall and, as a result, passive type earth pressure conditions take place on its hanging wall side leading to the formation of an easily observable failure wedge (L2). The consequent cofferdam displacement and rotation shears the soil on its footwall side facilitating the formation and propagation of a second rupture (L3) with quite lower dipping angle. In the second stage of faulting, $h > 0.2$ m, fault movement propagates simultaneously upon both rupture planes.
Extensive soil failure and shearing around the cofferdam, on both sides as well as its bottom, naturally leads to a dramatic increase in its rotation, in comparison to the previously discussed location. This is reflected on the rotational movement of the footing standing atop (Figure 5c). More importantly, the presence of the cofferdam substantially deteriorates the performance of the system in this position. The cofferdam-supported footing experiences about 3 times larger rotation than the alternative with no soil improvement. However, it should be observed that the cofferdam enhances the ability of the soil to sustain footing rotation without total failure and prevents overturning of the structure, which takes place for quite lower rotation amplitudes in its absence (Figure 5c). Undesirable as it may be, this was a predictable outcome captured with sufficient accuracy by the numerical analyses (Figures 5b and 5c). The discrepancy between analytical prediction and experiment regarding rotational footing movement (Figure 5c) is attributed to the aforementioned neglect of $P - \delta$ effects.

5. CONCLUSIONS

This paper has presented a combined experimental and numerical study of reverse fault rupture interaction with hybrid foundation systems. Motivated by promising results regarding their dynamic response, 1-g physical model tests investigated the effect of constructing a cofferdam structure under a rocking isolated footing. The key conclusions can be summarized as follows:
1) Cofferdams can impose kinematic constraints that may significantly alter the free field rupture pattern, causing diversion, bifurcation, and diffusion. The exact mechanism as well as the consequent response of the supported footing strongly depend on the location of the foundation with respect to the fault outcrop. As a result, the effectiveness of this hybrid foundation solution proved to be very sensitive to its exact location.
2) A nonlinear 3D FE method was developed, based on the model proposed by Anastasopoulos et al. (2007) and validated against successful Class-A predictions. This method enables parametric investigation of the response of similar hybrid foundation systems with respect to the key parameter of relative to the fault location. Given that it is impossible to predict the fault outcropping location with

sufficient accuracy, even in the case of documented active faults, design can only rely on numerically computed response envelopes of distress measures, such as displacement and rotation.

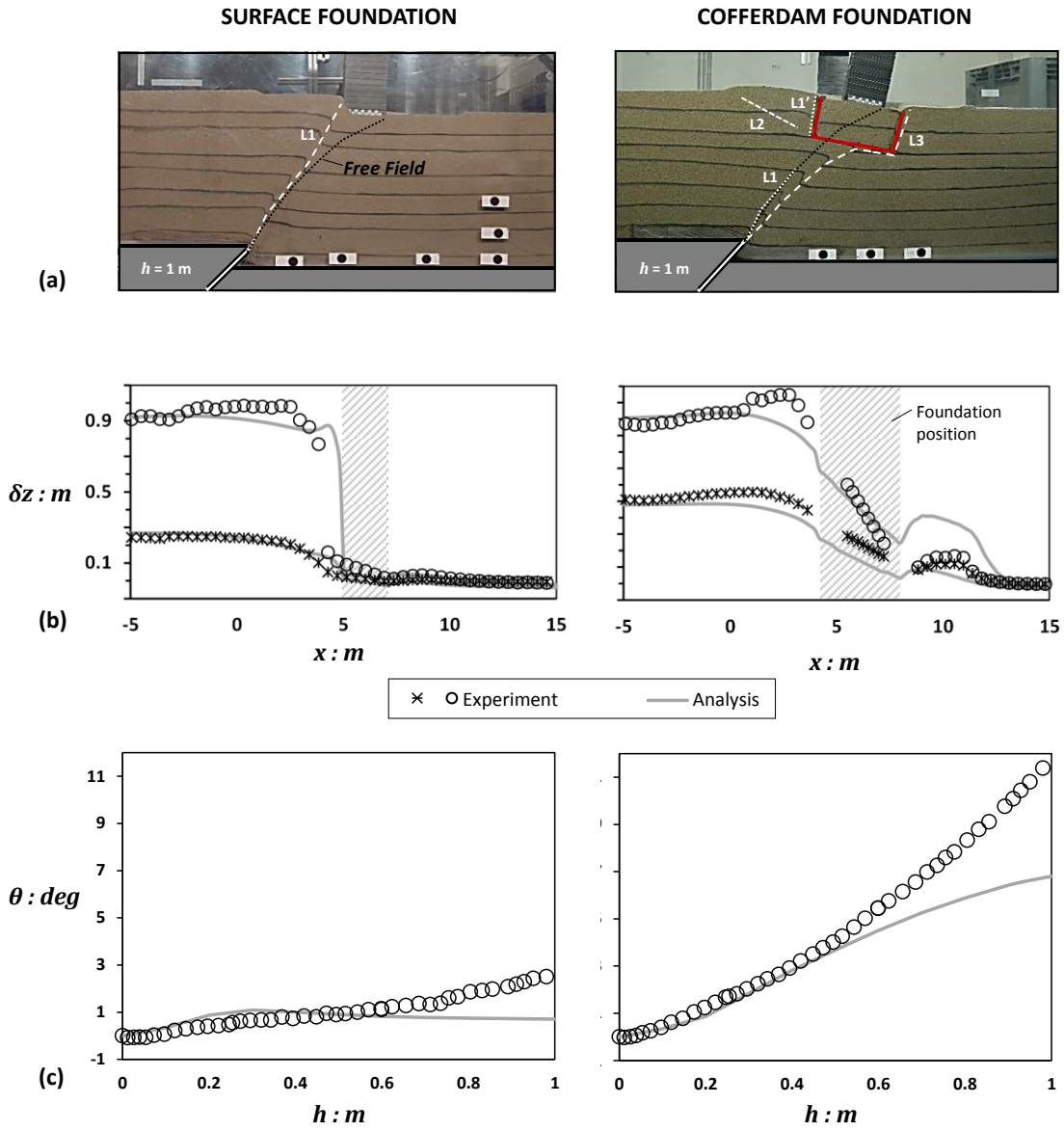

Figure 5. Response of a structure supported upon a hybrid footing–cofferdam foundation (right) in comparison to the benchmark surface foundation solution (left) for h = 1 m and relative to the fault position s/B = 0.8: (a) photos of the respective physical models; (b) experimental vs. analytical surface displacement profiles; and (c) evolution of foundation rotation in the experiment compared to the analysis.

7. REFERENCES

Ahmed W, Bransby MF (2009). The interaction of shallow foundations with reverse faults. *Journal of Geotechnical and Environmental Engineering* 135(7): 914-924.

Anastasopoulos I, Gazetas G (2007). Foundation-Structure Systems over a Rupturing Normal Fault: Part I. Observations after the Kocaeli 1999 Earthquake. *Bulletin of Earthquake Engineering*, 5(3): 253–275.

Anastasopoulos I, Gazetas G, Bransby MF, Davies MCR, El Nahas A (2007). Fault Rupture Propagation through Sand: Finite Element Analysis and Validation through Centrifuge Experiments. *Journal of Geotechnical and Geoenvironmental Engineering*, ASCE, 133(8): 943–958.

Anastasopoulos I, Gazetas G, Drosos V, Georgarakos T, Kourkoulis R (2008). Design of bridges against large tectonic deformation. *Earthquake Engineering and Engineering Vibration*, 7: pp. 345–368.

Anastasopoulos I, Gazetas G, Bransby MF, Davies MCR., El Nahas A (2009). Normal Fault Rupture Interaction with Strip Foundations. *Journal of Geotechnical and Geoenvironmental Engineering*, ASCE, 135(3): 359-370.

Anastasopoulos I, Gazetas G, Loli M, Apostolou M, Gerolymos N (2010). Soil failure can be used for seismic protection of structures. *Bulletin of Earthquake Engineering*, 8(2): 309-326.

Bransby MF, Davies MCR, El Nahas A, Nagaoka S (2008). Centrifuge modelling of reverse fault-foundation interaction. *Bulletin of Earthquake Engineering*, 6(4): 607-628.

Chang K-C, Chang D-W, Tsai M-H, Sung Y-C (2000). Seismic performance of highway bridges. *Earthquake Engineering and Engineering Seismology*, 2(1): 55-77.

Deng L, Kutter B, Kunnath S (2012). Centrifuge modeling of bridge systems designed for rocking foundations. *Journal of Geotechnical and Geoenvironmental Engineering*, ASCE, 138(3): 335–344.

Dong J.J., Wang C.D., Lee C.T., Liao J.J., Pan Y.W. (2003). The influence of surface ruptures on building damage in the 1999 Chi-Chi earthquake: a case study in Fengyuan City. *Engineering Geology*, 71:157–179.

Drosos V., Georgarakos T., Loli M., Anastasopoulos I., Zarzouras O., and Gazetas G. (2012). Soil–Foundation–Structure Interaction with Mobilization of Bearing Capacity: An Experimental Study on Sand. *Journal of Geotechnical and Geoenvironmental Engineering*, ASCE, 138(11): 1369–1386.

Faccioli E., Anastasopoulos I., Callerio A., Gazetas G. (2008), "Case histories of fault–foundation interaction," Bulletin of Earthquake Engineering, 6, pp. 557–583.

Fadaee M., Ezzatyazdi P., Anastasopoulos I., Gazetas G. (2016). Mitigation of reverse faulting deformation using a soil bentonite wall: Dimensional analysis, parametric study, design implications. *Soil Dynamics and Earthquake Engineering*, 89: 248–261.

Gajan S., Kutter B.L. (2009). Contact interface model for shallow foundations subjected to combined loading. *Journal of Geotechnical and Geoenvironmental Engineering*, ASCE, 135(3): 407–419.

Gelagoti F., Kourkoulis R., Anastasopoulos I., Gazetas G. (2012). Rocking Isolation of Frame Structures Founded on Separate Footings. *Earthquake Engineering & Structural Dynamics*, 41(7): 1177-1197.

Kawashima K. (2001). Damage of Bridges Resulting from Fault Rupture in The 1999 Kocaeli and Duzce, Turkey Earthquakes and The 1999 Chi-Chi, Taiwan Earthquake. Workshop on Seismic Fault-Induced Failures–Possible Remedies for Damage to Urban Facilities, University of Tokyo Press: 171-190.

Loli M., Anastasopoulos I., Bransby M.F., Waqas A., Gazetas G. (2011). Caisson Foundations subjected to Reverse Fault Rupture: Centrifuge Testing and Numerical Analysis. *Journal of Geotechnical and Geoenvironmental Engineering*, ASCE, 137(10): 914–926.

Loli M., Knappett J.A., Brown M.J., Anastasopoulos I., Gazetas G. (2014). Centrifuge modeling of rocking–isolated inelastic RC bridge piers. *Earthquake Engineering & Structural Dynamics*, 43(15): 2341-2359.

Loli M. (2015). *Non-linear Seismic Interaction Between Soil and a Slender Structure*. PhD Thesis, National Technical University of Athens.

Loli M, Gazetas G. (2017). Physical and Numerical Modelling of Hybrid Foundations to Mitigate Seismic Fault Rupture Effects, *Journal of Geotechnical and Geoenvironmental Engineering*, ASCE, under review.

Meyerhof G.G. (1951). The ultimate bearing capacity of foundations. *Géotechnique*, 2(4): 301–332.

Muir Wood D. (2004). *Geotechnical modelling*. Spon Press, London.

Pamuk A., Kalkan E., Ling H.I. (2005). Structural and geotechnical impacts of surface rupture on highway structures during recent earthquakes in Turkey. *Soil Dynamics & Earthquake Engineering*, 25(7): 581-589.

Paolucci R., Yilmaz, M.T. (2008). Simplified theoretical approaches to earthquake fault rupture–shallow foundation interaction. *Bulletin of Earthquake Engineering*, 6(4): 629-644.

White D.J., Take W.A., Bolton M.D. (2003). Soil deformation measurement using particle image velocimetry (PIV) and photogrammetry. *Géotechnique*, 53(7): 619-631.

Yilmaz M.T., Paolucci R. (2007). Earthquake fault rupture–shallow foundation interaction in undrained soils. *Earthquake Engineering and Structural Dynamics*, 36(1): 101–118.

Youd T.L., Bardet J.P., Bray, J.D. (2000). Kocaeli, Turkey, Earthquake of August 17, 1999 Reconnaissance Report. *Earthquake Spectra*, S1: 1-461.